BIOREACTOR AND SMALL MOLECULE DRUG APPLICATIONS IN HAIR CELL DIFFERENTIATION

By

SYLVIA YIP

A thesis submitted to the

School of Graduate Studies

Rutgers, The State University of New Jersey

In partial fulfillment of the requirements

For the degree of

Master of Science

Graduate Program in Cell and Developmental Biology

Written under the direction of

Kelvin Y. Kwan

And approved by

_____

_____

_____

_____

New Brunswick, New Jersey

October 2021

ABSTRACT OF THE THESIS

Bioreactor and Small Molecule Drug Applications in Hair Cell Differentiation

By SYLVIA YIP

Thesis Director:

Kelvin Kwan

Hair cells are mechanoreceptors of the inner ear that convert sounds into electrical signals to be perceived by the brain. The gradual loss of hair cells is common after a lifetime of chronic exposure to loud noises. Mammalian hair cells lack the ability to regenerate after embryonic development. Advancements in regenerative medicine strategies have been employed to restore function to damaged organs. The use of stem cells can regenerate and replace damaged hair cells. Understanding how stem cells differentiate into hair cells will provide insight into regeneration. To study hair cell regeneration, we employed an inner ear organoid system. Immortalized multipotent otic progenitor (iMOP) cells that differentiate into spiral ganglion neurons, supporting cells, and hair cells were used to generate organoids. This study tests whether a bioreactor facilitates sensory epithelial differentiation. The bioreactor agitates the medium to promote nutrient diffusion in the cultures. After ten days of differentiation, iMOP-derived organoids were collected, and relative changes in transcripts and protein markers that correspond to neurons, supporting cells, and hair cells were determined. The use of a bioreactor increased the percentage of cells expressing MYO6, a hair cell marker. The percentage of TUBB3 labeled neurons also increased while GFAP labeled supporting cells remained the same. Relative levels of *Myo6* mRNA did not increase in any of the culture conditions while relative levels of *Tubb3* mRNA significantly increased in all cultures compared to control samples.

Although molecular mechanisms are unknown, the study shows that use of the bioreactor improves hair cell differentiation in otic progenitor-derived organoids.

ACKNOWLEDGEMENTS

I am extremely grateful to my thesis advisor Dr. Kelvin Kwan for his guidance and encouragement. I have been with his laboratory since my undergraduate days, and he has been a phenomenal mentor since the beginning. I very much appreciate the whole Kwan lab for their constant support, especially undergraduates Alyssa Ferdinand and Michael Lau for their assistance with data quantification. I would also like to thank Azadeh Jadali for their expertise and advice in cell culture work. In addition, I want to extend my gratitude to my defense committee: Dr. Gabriella D'Arcangelo, Dr. Kristen Labazzo, and Dr. Peng Jiang for their time and valuable input. Last but not least, I am thankful for all of my family and friends that supported me in every step throughout my time at Rutgers!

Table of Contents

Table of Figures and Tables

Chapter 1: Introduction

1.1 Properties of Pluripotent Stem Cells

Union of the sperm and egg during fertilization forms a one cell embryo - the zygote- that starts embryonic development. The zygote undergoes cell division and cell specification to form a multicellular organism composed of a myriad of different cell types. The zygote is totipotent and can develop into cells of the three germ layers as well as trophectoderm, the extraembryonic cells of the placenta. As development proceeds, the zygote undergoes rapid mitotic division, and the differentiation potential begins to decrease[1]. Rapid cell division of the zygote leads to the formation of a hollow ball of cells called the blastocyst. Cells in the blastocyst are composed of an outer layer of cells called the trophoblast. The layer of trophoblasts surrounds the inner cell mass in a fluid filled cavity. Cells from the trophoblast give rise to the placenta, while cells from the inner cell mass contain pluripotent cells that differentiate into tissues of the three primary germ layers: endoderm, ectoderm, and mesoderm[2]. Embryonic stem cells (ESCs) derived from the inner cell mass are self-renewing undifferentiated cells that have the capability to develop into cells of the three germ layers *in vitro* and *in vivo*. At the end of gastrulation, the ESCs differentiate into distinct cell lineages and initiate organogenesis (**Figure 1**) [3].

Adult somatic stem cells are found in the mature brain, bone marrow, intestines, and many more organs. In contrast to ESCs, somatic stem cells are multipotent and have limited differentiation potential[4]. They can only develop into restricted cell types. For example, neural stem cells are multipotent and give rise to cells of the nervous system

such as neurons. In the adult organism, somatic cells are terminally differentiated. Somatic cells, however, can be reprogrammed into induced pluripotent stem cells (iPSCs). iPSCs are embryonic-like stems cell that display properties of self-renewal and pluripotency. These cells were first generated by overexpressing four transcription factors: c-MYC, KLF4, OCT4, SOX2[5]. Expression of these factors reprogram cells at the epigenetic level to give rise to cells that are similar to ESCs. Since this initial finding, employment of different combinations of genes, small molecules, and other factors have also generated iPSCs. ESCs and iPSCs have properties of self-renewal and pluripotency as well as similar transcriptome[6].

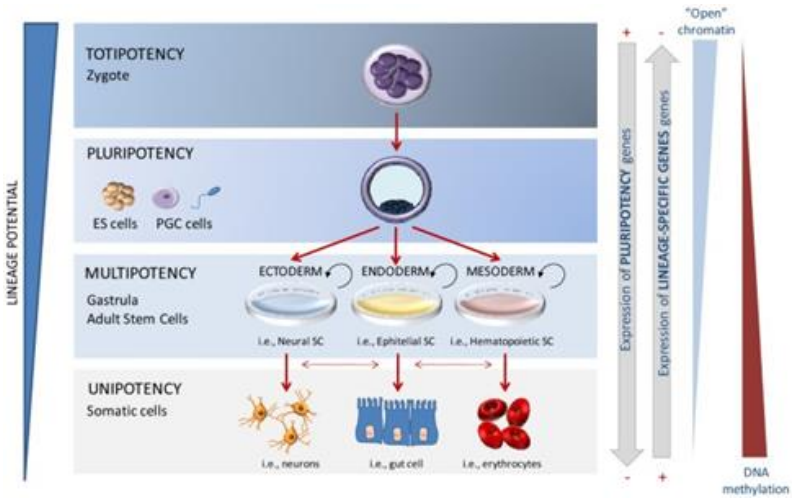

Fig. 1 The hierarchy of stem cell potency.

One major difference between terminally differentiated somatic cells and pluripotent stem cells is continual cell division. Cell cycle progression drives cell division. The phases of the cell cycle progression depend on formation of distinct cyclin and cyclin dependent kinase complexes. Cyclins regulate the cell cycle by binding to cyclin dependent kinases (CDKs). Cyclins are cyclically expressed, and their protein

levels fluctuate throughout the cell cycle. CDK levels do not vary as much throughout the cell cycle. Cyclins can be classified into four main classes: G1, G1/S, S, and M[7]. Active CDKs are phosphorylated and form a protein complex with cell cycle specific cyclins. The activated cyclin-CDK complexes phosphorylate proteins to activate them in order to coordinate cell cycle progression and mitosis. Cyclin E, D, and A are involved in transitioning from the G1 to S phase by binding to CDK 2, 4, and 6 respectively.

CDK2 has a role in self-renewal and proliferation for neural progenitors. A study indicated CDK2 knockout mice displayed aberrant neural progenitor differentiation and decreased cell proliferation[8]. The results suggested that perturbing the G1/S transition not only affects cell cycle progression but also affects differentiation. Normally, during differentiation, the G1 phase lasts longer, concomitant with decreased CDK1 and CDK2 activities[9]. These results suggest that a longer G1 phase allows accumulation of necessary factors that promotes differentiation. In contrast, a shorter G1 phase promotes self-renewal and maintains pluripotency.

The potential for stem cells to self-renew or differentiate is intimately linked to cell division. Two modes of cell division have been observed **(Figure 2)**[10]. Symmetric division yields identical daughter cells: two stem cells or two differentiated stem cells. The rise of two daughter stem cells can expand the stem cell population[11]. In sharp contrast, asymmetric cell division yields one stem cell and one differentiated cell[12]. The type of cell division is dependent on intrinsic and extrinsic signals from the local microenvironment such as the stem cell niche. Intrinsic signals can induce an unequal distribution of self-renewal and differentiation factors in daughter cells. Stem cells that remain in close contact with the niche are exposed to extrinsic signals that can affect

pluripotency and differentiation[13]. Both intrinsic and extrinsic signals influence stem cell fate.

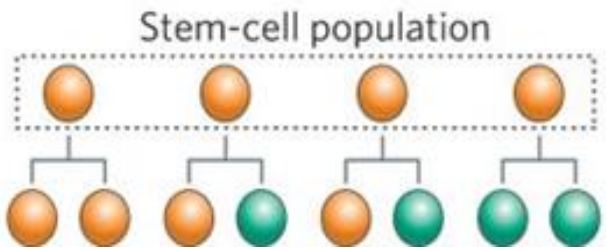

Fig. 2 Symmetric and asymmetric stem cell division.

Somatic stem cells usually reside in a quiescent state and are only activated by injury or to maintain homeostasis. For instance, hematopoietic stem cells replicate about every 25-50 weeks to maintain blood cell production[14]. While stem cells can repair and renew old tissue, the potential to regenerate declines with age. In sensory systems, such as the inner ear, there are no somatic stem cells. The emerging field of regenerative medicine investigates ways to utilize stem cells or lineage restricted progenitors to treat diseased and damaged tissue.

1.2 Cell Replacement Applications Using Pluripotent Stem Cells

The ultimate goal of regenerative medicine is to replace cells in damaged tissues and organs. The application of stem cell therapy can ideally restore lost function due to damaged cells. Stem cells can be used in lieu of organ transplantation. This method allows the stem cells to differentiate into the cell types necessary to repair or replace the damaged organ. ESCs were initially proposed for use in stem cell therapy treatment and disease modeling. The first-in-human ESC treatment was approved by the U.S. Food and Drug Administration in 2009 to treat spinal cord injury patients[15]. However, the

controversial nature of attaining ESCs from early stage human embryos causes ethical concerns. Use of iPSCs as an alternative bypasses the need for using human embryos since these cells can be generated from adult somatic cells. Patient-derived iPSCs also avoid potential immune rejection after transplantation. In 2014, the first clinical trial using iPSC treatment in humans went underway. Autologous iPSCs were differentiated into retinal pigment epithelial cells that were then transplanted into the patient with macular degeneration of the eye[16]. No signs of rejection or tumorigenicity occurred in the patients[17]. The outcome and safety of this trial reassured the use of iPSCs in treating diseases. Currently, there are many iPSC clinical trial studies ongoing worldwide.

Stem cells obtained from patients with congenital diseases can also be used for human disease modeling. These studies can help better understand causes, treatments and transmission of diseases[18]. Both ESCs and iPSCs were used for Fragile X syndrome (FXS) disease modeling. FXS is caused by mutations in the fragile X mental retardation 1 (*FMR1*) gene. The fragile X mental retardation protein (FMRP) is necessary for proper brain development. The lack of proper FMRP impairs brain development and causes learning disabilities. ESCs from an affected embryo were used to create an FXS model to study the developmental disorder. iPSCs were created by reprogramming somatic cells from FXS diagnosed patients and differentiated into neurons. Use of iPSCs was effective in studying morphological phenotypes of FXS neurons[19]. ESC and iPSC models are beneficial for studying different aspects of FXS.

Regenerative medicine applications can benefit those who suffer from hearing impairments. Age-related hearing loss is a prevalent yet underappreciated disorder that affects over 15% of the population by the age of 18[20]. A major cause of age-related

hearing loss is the degeneration of hair cells and spiral ganglion neurons of the inner ear. Current treatments such as hearing aids still rely on remaining hair cells, while functioning spiral ganglion neurons are required for cochlear implants. Without a threshold number of hair cells or SGNs, current treatments using auditory prosthesis are futile. To effectively treat hearing loss, we need to understand how the inner ear works and how hair cells and SGNs are normally generated during development. By understanding the underlying molecular process responsible for differentiation of these cell types will shed light on the regeneration process. These results will help us better design strategies to treat hearing loss and open the door for further research that might one day lead to treatments for auditory neuropathies and alleviate deafness.

1.3 Function and Development of the Inner Ear

Sound waves traveling through the air are collected by the pinna or the outer ear. The sounds are then funneled through the ear canal and impinge on the eardrum or the tympanic membrane. Movement of the tympanic membrane sets in motion the middle ear bones, the malleus, incus, and stapes to amplify movements of the tympanic membrane[21]. The stapes impinges on the oval window which sets in motion the fluid in the cochlea to generate a traveling wave. The traveling wave causes the basilar membrane to vibrate in the cochlea. The organ of Corti located in the cochlea contains hair cells, the auditory receptors of the inner ear[22]. These mechanoreceptors convert the mechanical vibrations of the basilar membrane into electrical signals.

Hair cells have protrusions that extend from the apical surface called stereocilia. Each hair cell has 50 to 100 stereocilia arranged by ascending height in a staircase profile

to form a hair bundle. The tips links of stereocilia contain filaments that adjoin stereocilia to its taller adjacent neighbor[23]. The lower end of the tip links are connected to mechanically-gated transduction channels. Vibration of the basilar membrane pushes the hair cell up and deflects the hair bundle on an overlying membrane called the tectorial membrane. Deflection of the hair bundle towards the tallest stereocilia increases tension in the tip links and opens the hair cell transduction channel. An influx of cations composed mainly of K^+ ions enters the ion channel and depolarizes the cell. Depolarization of the hair cell opens voltage-gated calcium channels at the base of the hair cell. The influx of Ca^{2+} ions prompts vesicular fusion and release of neurotransmitters into the synaptic cleft where the nerve terminal resides[24]. Binding of the neurotransmitter to receptors at the neuronal terminal depolarizes the membrane to initiate an action potential. The auditory nerve then transmits the action potential as a neural signal to the brain which is interpreted as sound (**Figure 3**)[24].

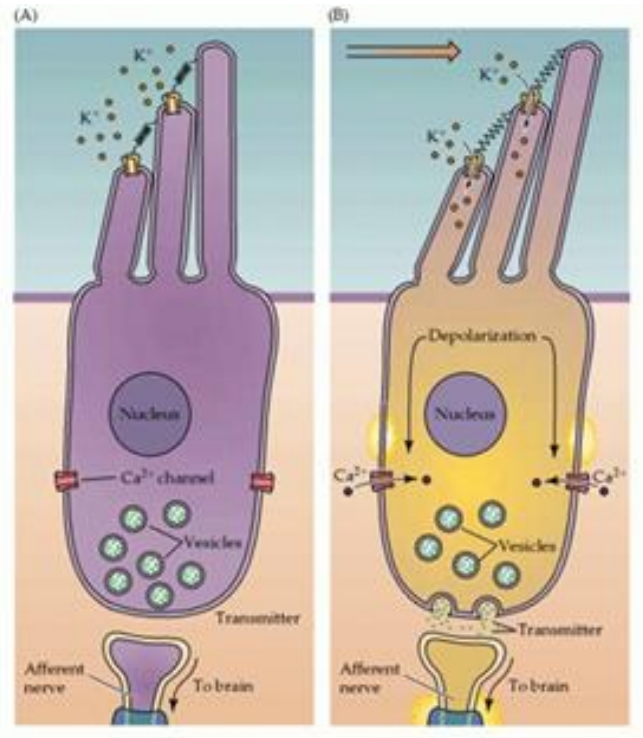

Fig. 3 Depolarization of a hair cell. (A) Hair bundles deflecting towards the tallest stereocilia allows an influx of K^+ ions. (B) The depolarization of the hair cell allows an influx of Ca^{2+} ions and the release of neurotransmitters to nerve endings.

Inner ear formation begins with the thickening of the ectoderm to form the otic placode[25]. The otic placode invaginates to form the otic cup and undergoes morphological changes. As development proceeds, the otic cup closes to form the otic vesicle. Neurosensory progenitors from the anteroventral region of the otic vesicle are specified by SOX2. These progenitors give rise to neurons and hair cells of the inner ear[26]. Neurogenin1 (NEUROG1) and atonal homolog 1 (ATOH1) are basic helix-loop-helix transcription factors that further specify neuronal and hair cell lineages. The expression of NEUROG1 initially establishes neurosensory progenitors that are competent to become neurons or sensory cells. As inner ear development proceeds, the neuronal progenitors delaminate from the otic placode and leave behind sensory

progenitors that give rise to hair cells and supporting cells[27]. During establishment of these cell types, SOX2 activates expression of both NEUROG1 and ATOH1[28]. Downregulation of SOX2 allows ATOH1 expression. Additional transcript factors, including NEUROG1, have a proposed role in repressing ATOH1 expression. In line with the hypothesis, NEUROG1 null mice were observed to have fewer neurons and smaller sensory epithelia[29]. It is proposed that NEUROG1 may prevent ATOH1 expression through transcriptional, post-transcriptional or post-translational mechanisms[25]. The gene regulatory networks between NEUROG1 and ATOH1 are crucial for inner ear development (**Figure 4**)[28].

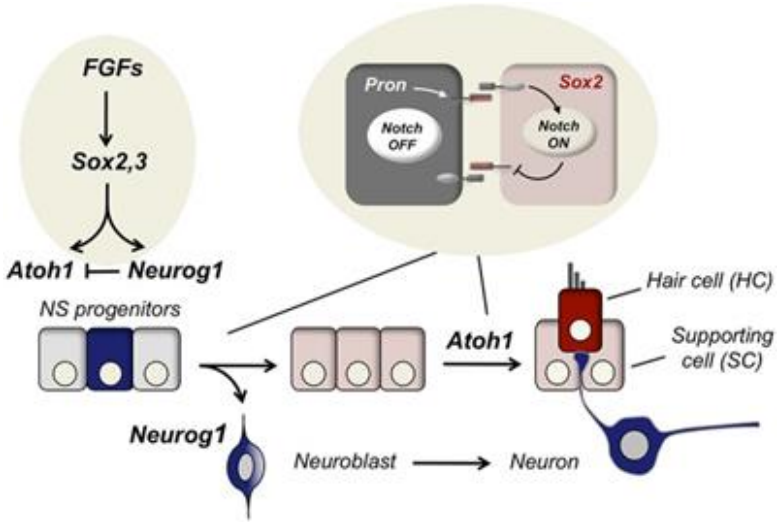

Fig. 4 Neuron and hair cell differentiation. NEUROG1 is expressed during neurogenesis. ATOH1 expression in sensory progenitors is delayed until after delamination of neuronal progenitors.

1.4 Hair Cell Regeneration

In adult mammals, hair cells cannot be regenerated. Permanent hearing loss occurs when loud sounds and ototoxic drugs kill hair cells. Unlike mammals, birds are capable of regenerating hair cells through cell cycle re-entry and transdifferentiation of supporting cells[30]. Recent advances in regenerative medicine show promising results in hair cell production. The expression of ATOH1 is downregulated after completion of inner ear development[31]. Re-expression of ATOH1 has been investigated in postnatal and adult mammals to promote mammalian hair cell regeneration. A modified adenovirus harboring ATOH1 was used as a vector for gene delivery and to re-express ATOH1 in the cochlea of a deafened guinea pig. Introduction of ATOH1 generated nascent hair cells and improved hearing in this model system[32]. Gene therapy holds promising results in restoring hearing loss.

Stem cells have the potential to differentiate into hair cells and be used to replace damaged or lost hair cells. Both ESCs and iPSCs can generate hair cells. Murine ESCs were used to generate inner ear progenitors from a stepwise differentiation protocol[33]. Integrated stem cell-derived progenitors at injured epithelia expressed hair cell markers and displayed hair bundles. Human iPSCs are also capable of being transformed into hair cell-like cells through *in vitro* stepwise differentiation[34]. However, the yield of hair cell-like cells was very low. While stem cell replacement has the potential to be used in transplant for hair cell replacement, current protocols cannot generate a substantial number of hair cells[35]. For stem cells to be used in regenerative medicine, optimized differentiation is required. There is a need to develop proper culture conditions to optimize the generation of new hair cells.

1.5 Study Overview

Immortalized multipotent otic progenitor (iMOP) cells are an otic-fate restricted cell line that can differentiate into neurons, supporting cells, and hair cells[36]. Although previous sensory epithelial differentiation conditions for iMOPs were established, we seek to improve on these conditions to promote hair cell differentiation. We propose that use of a bioreactor and a small molecule inhibitor of CDK2 (K03861) can further facilitate hair cell differentiation.

iMOPs are a fate restricted cell line derived from SOX2 expressing cochlear progenitors. Otospheres, aggregated otic cells, were obtained from E12.5 murine cochlea and transduced with a *c-Myc* retrovirus. The transient expression of C-MYC amplified SOX2-dependent transcription of genes involved in self-renewal[37]. Through this method,

a fate restricted cell line was generated with self-renewing properties. iMOP cultures are treated with bFGF to stimulate proliferation. Otospheres have the potential to differentiate into multiple cell types such as spiral ganglion neurons, supporting cells, and hair cells. Withdrawal of growth factor decreases proliferation, facilitates cell cycle exit and promotes differentiation[31].

iMOP derived sensory epithelial cultures contain a heterogenous population of cells. This includes cells at different stages of developing neuron, supporting cell, and hair cell. They can be distinguished by different protein markers. Each individual cell can differ extensively from the other surrounding cells. For instance, a developing neuron has neurites that extend from the cell body. Class III β-tubulin (TUBB3) is a component of microtubules found primarily in the neurites. TUBB3 regulates microtubule organization and is necessary for extension of axonal processes[38]. Glial fibrillary acidic protein (GFAP) is an intermediate filament protein expressed in supporting cells and glial cell types such as astrocytes[39]. GFAP is incorporated into the cytoskeleton to give structural support to a cell. Myosin VI (MYO6) is a motor protein that binds to actin. MYO6 is present at the base of actin filaments in stereocilia as well as in the hair cell body. It is suggested that MYO6 anchors stereocilia rootlets to the cuticular plate, an actin mesh that resides below the hair bundle[40]. These markers can be used to classify different cell types in a heterogenous population.

The use of a bioreactor device can facilitate organoid differentiation. The microenvironment is essential for cell growth and differentiation. An issue in differentiating stem cells *in vitro* is the lack of vasculature[41]. During mammalian embryonic development, the placenta and blood vessels deliver oxygen and nutrients to

the growing embryo. When cells are differentiated *in vitro*, there is no efficient means of oxygen or nutrient delivery to cells that reside in the center of the otosphere. A bioreactor may facilitate delivery of oxygen and nutrients to the cells[42]. Neural stem cells are noted to differentiate more efficiently into neurons and oligodendrocytes in microfluidic channels that facilitate delivery of growth factor[43]. We hypothesize that use of a miniaturized bioreactor will stimulate nutrient diffusion into iMOPs.

Addition of K03861 in otic progenitors has been shown to enrich post-mitotic cells that are primed differentiation. This small molecule has been used to increase the percentage of cells with neuronal morphology in iMOP cultures[44]. As previously stated, the interplay between CDK and cyclins are pivotal for stem cell fate regarding proliferation and differentiation. K03861 inhibits CDK2 kinase activity by interfering with the formation of cyclin-CDK complexes[45]. The use of K03861 has been tested on neuronal differentiation but not on sensory epithelial differentiation.

We will test the hypothesis that use of a bioreactor and K03861 for culturing iMOP-derived organoids will facilitate sensory epithelial differentiation. A total of four conditions will be tested. 1) Control conditions where cells are cultured in suspension. 2) Addition of K03861 in suspension cultures to enrich post-mitotic cells primed for differentiation. 3) Suspension cultures grown in bioreactors and finally 4) suspension cultures grown in bioreactors with the addition of K03861. To determine the effects on sensory epithelial differentiation, organoids will be collected after ten days of culture for quantitative reverse transcription PCR (RT-qPCR) and fluorescent immunostaining. Statistics will be applied to analyze the results to validate the optimal conditions, and to better understand sensory epithelial differentiation conditions.

Chapter 2: Materials and Methods:

2.1 Spinfinity (Miniaturized Bioreactor) Assembly

Design files for 3D printed parts and the 5Motors python script were as published[46]. Parts were printed with high temperature resin at Rutgers Makerspace, sterilized with 70% ethanol and exposed to UV lighting for 24 hours (**Figure 5**). The Python 5 Motors.py is a python script that controls the speed of the motor and paddles. The printed, hardware, and electrical components are listed in Table 1.

Quantity	Part	Label in Fig .5
1	12-Well Plate Lid	A-4
1	Acrylic Sheet	A-2
1	Base	A-8
6	Counterclockwise Paddles	A-7
6	Clockwise Paddles	A-7
11	Gears	A-5
1	L298N Motor Drive Controller Board	A-6
1	Motor 10 RPM, 12 V	A-1
1	Motor Shaft Gear	A-5
12	PTFE collars	A-4
1	Raspberry Pi 3 A+	A-3
1	Raspberry Pi 3 A+ power supply	Not shown
1	Raspberry PiTM 16 GB MicroSD NOOBS Card	Not shown
1	Raspberry Pi LCD 7” Touchscreen	A-3

Table 1 Quantity and components of the bioreactor.

Organoids are cultured in a 12-well cell culture plate held by the Base. The 12-Well Plate Lid is used instead of the lid of the cell culture plate. This printed lid holds the PTFE collars. Counterclockwise (CW) and Clockwise (CCW) Paddles are inserted through the PTFE collars. The propellers on the paddles are submerged into the culture

media. Paddles are arranged in an alternating pattern of CW and CCW to spin in their assigned direction. Gears and the Motor Shaft Gear rotate the paddles under the motor's control. The Motor Shaft Gear is connected to the motor and rotates the surrounding gears. A laser cutter was used to cut the acrylic plate. The cut plate holds the motor in place. 45- and 35-mm Hexes, M3 Washers, and M3 Hex Nuts support and fasten individual parts of the bioreactor together. About 3 feet of 2 wire cable was soldered onto the motor. A male JST plug was crimped onto the wires. The motor connects to the Raspberry Pi 3A+ and L298N Motor Drive Controller Board. The driver controls the speed and direction of the DC motor. The touchscreen allows human interaction to input commands (**Figure 5**).

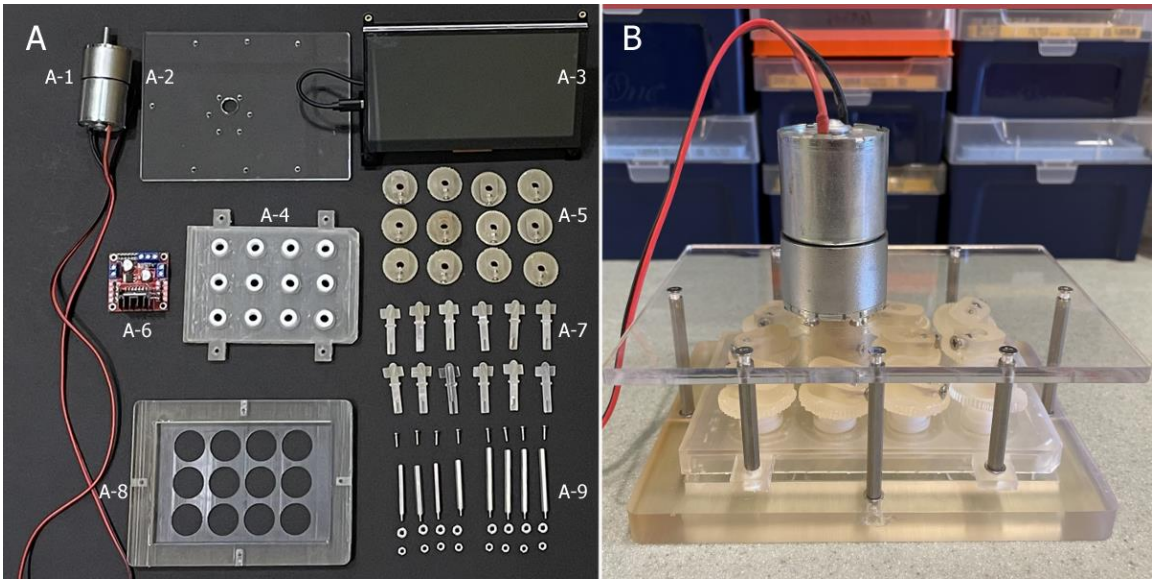

Fig. 5 Spinfinity: a miniaturized bioreactor. (A) 3D printed and hardware components of the bioreactor. (B) Fully assembled bioreactor.

2.2 iMOP maintenance

Culture medium consisted of DMEM/F12, 1X N21 supplement, 25 µg/ml carbenicillin and 20 ng/ml bFGF was used to maintain iMOP cells. Medium was added to cells every other day. Cells were passed every 5 to 7 days. Cells were harvested by gravity sedimentation and dissociated into single cells with TrypLE express. After washing with HBSS containing Mg^{+2} and Ca^{+2}, $1x10^6$ cells were plated in a 6 cm dish with culture medium and incubated at 37°C with 5% CO_2.

2.3 Sensory Epithelial Differentiation

1 x 10^5 cells were seeded into a single well of a 12 well plate. The multiwell plate allowed simultaneous testing of different culture conditions. Sensory epithelial media consisted of DMEM/F12, 1X N21-Max supplement, and 25 µg/ml carbenicillin. Sensory epithelial media with a small molecule consisted of DMEM/F12, 1X N21-Max supplement, 25 µg/ml carbenicillin and 1 µM K03861. The paddles from the bioreactor cultures were set at 10 revolutions per minute (rpm). Additional media was added on days 3 and 7.

2.4 Immunofluorescence

Otospheres were dissociated with TrypLE express for quantification. Intact otospheres were collected for morphological analysis. Both intact and dissociated cells were fixed with 4% formaldehyde for 30 minutes and washed with 1X PBS. Cells were then permeabilized with wash buffer (1X PBS containing 0.1% Triton X-100) and incubated in blocking solution (1X PBS containing 10% goat serum, and 0.1% Triton X-

100) to mitigate non-specific binding of antibodies for 1 hour at room temperature. Cells were incubated with primary antibodies against TUBB3, MYO6, and GFAP overnight at 4°C. Subsequently, intact otospheres were washed with wash buffer and dissociated cells resuspended in 1X PBS containing 0.1% Tween-20 to prevent reaggregation of cells if samples were not immediately used. Cells were incubated overnight with secondary antibodies in blocking solution at 4°C. After washes, cells were mounted onto slides with Prolong Gold Antifade (Thermo Fisher Scientific). For quantification, samples were prepared in triplicates and at least 100 cells per condition were counted using ImageJ. Hoechst labeled nuclei were used to identify individual cells. A threshold for background signal was established from samples that were incubated in secondary antibodies only.

2.5 RT-qPCR

Total RNA of three biological samples from each condition were extracted using the TRIzol reagent (Thermo Fisher Scientific). 1 mL of TRIzol was used to solubilize each sample. 0.2 mL of chloroform was used to lyse the cells. RNA quantity was measured with the NanoDrop Spectrophotometer. 1 μg of RNA was used to synthesize cDNA using the qScript cDNA synthesis kit (Quantabio). qPCR performed on the StepOnePlus real-time PCR machine was used to detect relative levels of mRNA from at least three biological replicates. Each biological sample included three technical replicates. SYBR green qPCR mix (Thermo Fisher Scientific) was used for qPCR reactions. Thermal cycler settings were set at 40 cycles of 95°C for 15 s, 60°C for 1 min. Housekeeping gene *Actb* was used as an internal control. Cycle threshold (Ct) values were obtained and the ΔΔCT method was performed to calculate gene expression compared to control samples. The primers used are listed in Table 2.

Gene	Forward primer	Reverse primer
Myo6	CAGATGGGCAATATTGTGG	GAACAGTTATCTTCCACATC
Tubb3	GTGGACTTGGAACCTGGAAC	TTCTCACACTCTTTCCGCAC
Gfap	CGGAGACGCATCACCTCTG	AGGGAGTGGAGGAGTCATTCG
Actb	GGCTGTATTCCCCTCCATCG	CCAGTTGGTAACAATGCCATGT

Table 2 Primers for qPCR

2.6 Statistical analysis

Fisher's exact test was conducted to test if the proportion of labeled cells were significant between different conditions. Since we hypothesize that the use of the bioreactor and inhibitor will facilitate sensory epithelial differentiation, pairwise comparisons were assessed to see if the proportion of labeled cells increased in the presence of K08361 and bioreactor. The Bonferroni correction was applied to account for the increased risk of Type I errors when conducting multiple comparison tests. The α value was adjusted from 0.05 to 0.0167 with the Bonferroni correction. Changes in gene expression were compared between different culture conditions using one-way analysis of variance (ANOVA) with post-hoc Tukey Honestly Significant Difference (HSD) tests at an α value of 0.05.

Chapter 3: Results

3.1 Cells from organoid cultures express hair cell, neuronal and glial markers

iMOP derived organoids were cultured for 10 days. During the course of differentiation, increase in the size and number of cells in the organoids can be observed (**Figure 6**). At the end of the differentiation period, organoids were collected for quantitative analysis. Cells were stained for neuronal marker TUBB3, supporting cell marker GFAP, and hair cell marker MYO6. Organoids from all four different conditions showed markers for all three cell types **(Figure 7)**. Images of immunofluorescently labeled organoids were acquired. The percentages of cells expressing different cell markers were assessed. Dissociated cells from organoids were used to unambiguously identify labeled cells in all culture conditions.

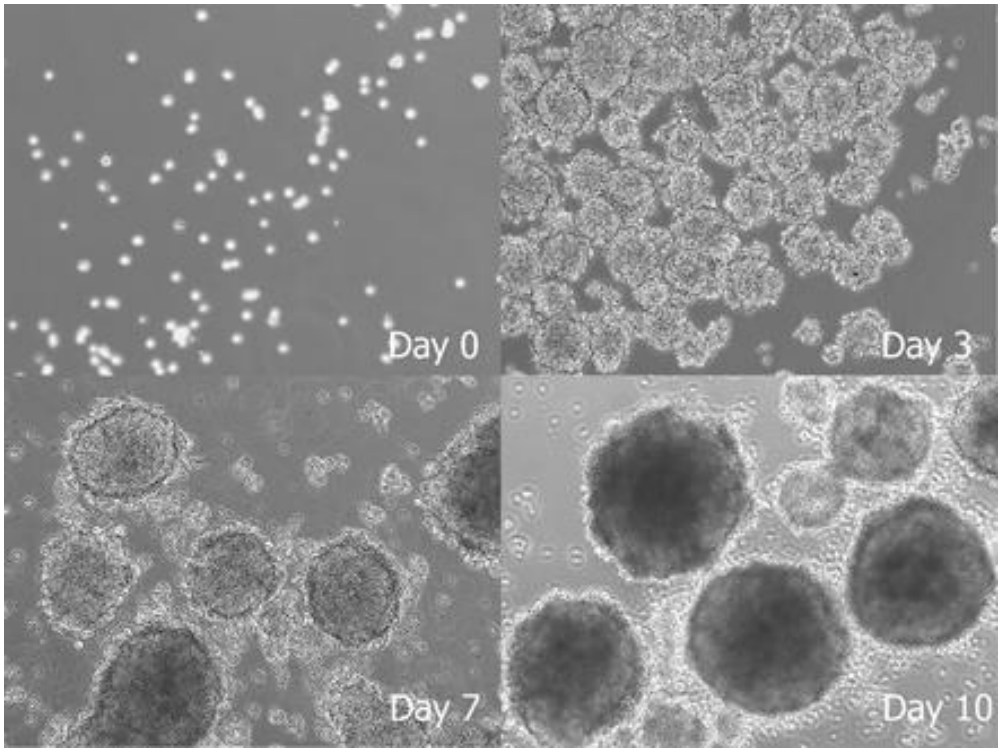

Fig. 6 Brightfield micrographs of iMOP-derived organoids undergoing differentiation. Different timepoints during differentiation are shown and labeled accordingly in each panel.

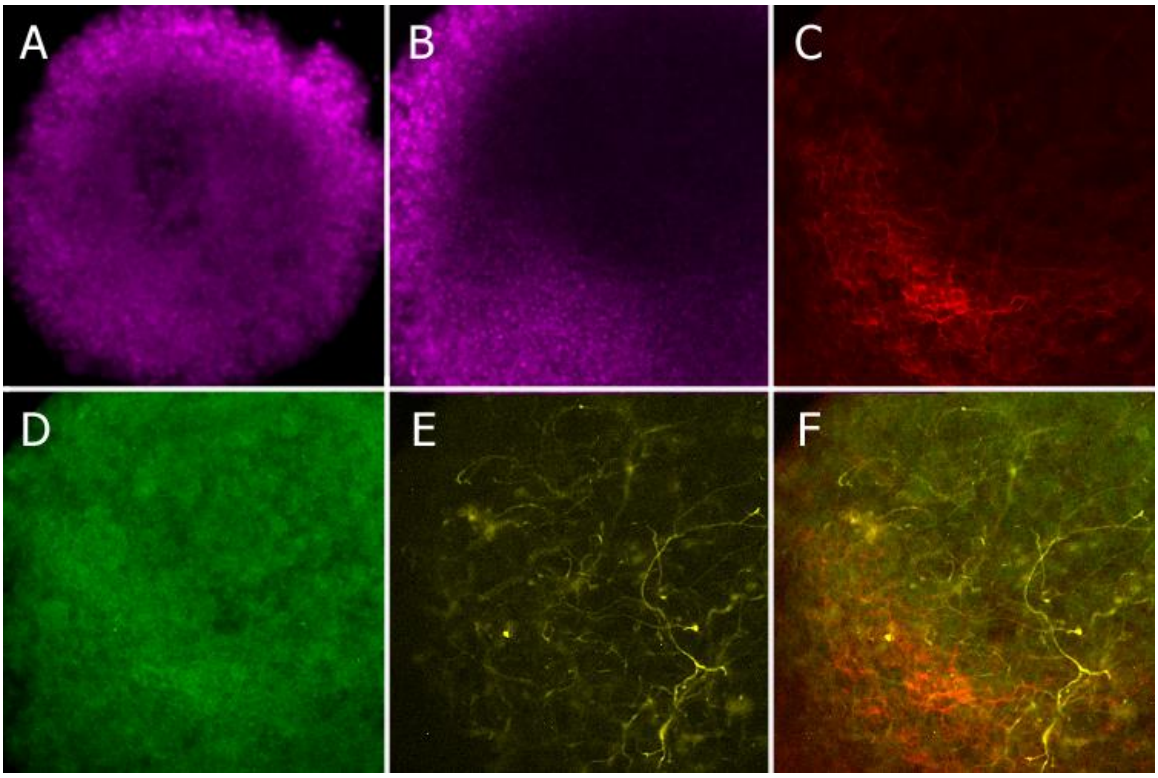

Fig. 7 Marker expression in organoids. (A) Otosphere stained for nuclei marker Hoechst. (B) Cells marked with Hoechst. (C) Neuronal marker TUBB3. (D) Hair cell marker MYO6. (E) Supporting cell marker GFAP. (F) Merged image of TUBB3, MYO6, and GFAP markers represent a heterogeneous population of different cell types obtained from organoids.

Use of bioreactor increases the proportions of MYO6 and TUBB3 labeled cells

Using immunofluorescent images, the proportion of labeled cells in different culture conditions were compared to control (cultures grown in suspension). The proportion of MYO6 labeled cells from the four conditions were evaluated using Fisher's exact test. The Bonferroni correction was applied with an adjusted $\alpha = 0.0167$ to reduce the occurrence of a Type I error (false positive). The use of the bioreactor showed a statistically significant increase of MYO6 labeled cells only in cultures without the inhibitor ($p<9.36 \times 10^{-3}$). The addition of K03861 or cultures grown in the bioreactor

with the addition of K03861 did not significantly increase MYO6 labeled cells (**Figure 8**).

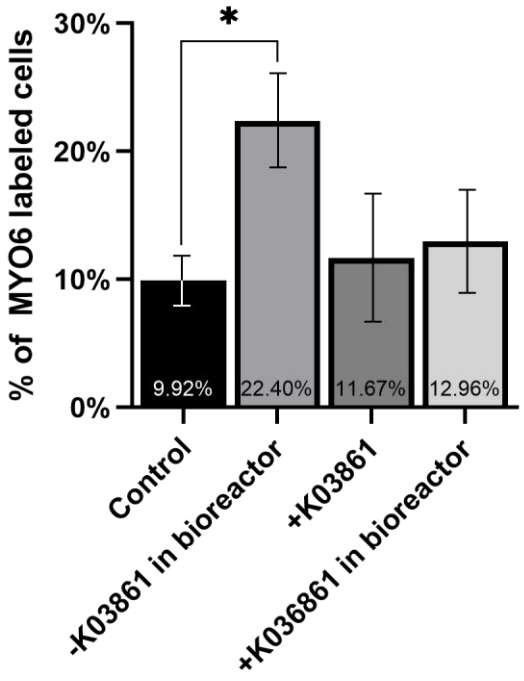

Fig. 8 Percentage of MYO6 labeled cells in different culture conditions. Control cultures had the lowest proportion of MYO6 labeled cells at 9.92±2.01%. Bioreactor cultures had the highest proportion of MYO6 labeled cells at 22.40±3.72%. Significant difference in proportions was detected with the use of a bioreactor ($p<9.36 \times 10^{-3}$) compared to control cultures. Error bars indicate standard error.

Since the bioreactor was able to facilitate hair cell differentiation, we were also interested in assessing neuronal and supporting cell differentiation. The proportions for TUBB3 and GFAP labeled cells were evaluated. The use of the bioreactor showed a significant increase of TUBB3 labeled cells ($p<8.79 \times 10^{-6}$). The addition of the K03861 or culture in the bioreactor with K03861 did not significantly increase the percentage of

TUBB3 labeled cells (**Figure 9**). No statistically significant changes in proportion of GFAP expressing cells were observed in any conditions (**Figure 10**).

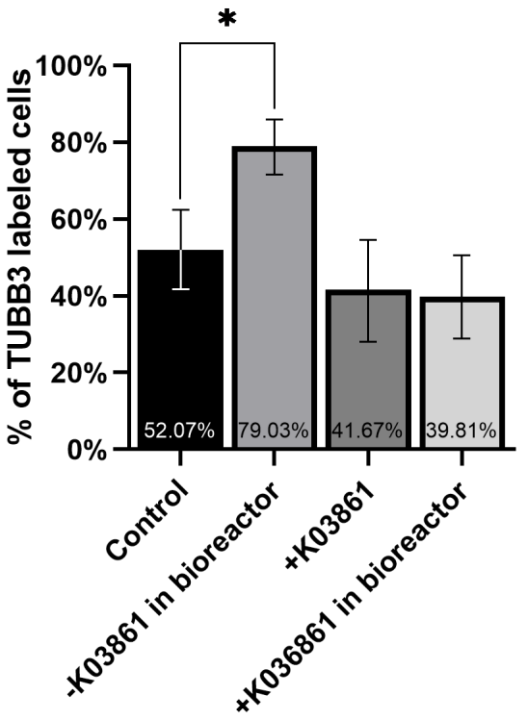

Fig. 9 Percentage of TUBB3 labeled cells in different culture conditions. The addition of K03861 in bioreactor had the lowest proportion of TUBB3 labeled cells at 39.81±11.05%. Bioreactor cultures had the highest proportion of TUBB3 labeled cells at 79.03±7.08%. Significant difference in proportions was detected between control and bioreactor cultures ($p<8.79 \times 10^{-6}$). Error bars indicate standard error.

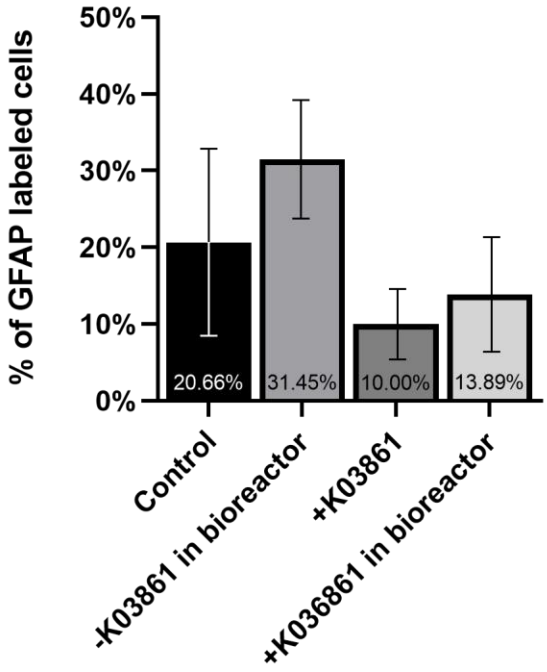

Fig. 10 Percentage of GFAP labeled cells in different culture conditions. The addition of K03861 had the lowest proportion of GFAP labeled cells at 10.00%±4.60%. Bioreactor cultures had the highest proportion of GFAP labeled cells at 31.45%±7.75%. No significant results were reported. Error bars indicate standard error.

3.2 Use of bioreactor and K03861 increases relative levels of *Tubb3* mRNA

Since translation and transcription are distinct macromolecular processes that ultimately regulate protein expression levels, mRNA levels were also assayed to determine if transcript changes correlate with protein changes. After 10 days in culture, mRNA expression of *Myo6*, *Tubb3* and *Gfap* were detected by RT-qPCR in cells from all four culture conditions. Compared to control cultures, *Myo6* and *Gfap* mRNA levels were not significantly upregulated under any conditions. Only *Tubb3* mRNA levels were increased. Comparison of *Tubb3* samples using One-way ANOVA indicated that there were significant differences in *Tubb3* mRNA expression levels ($p<6.16 \times 10^{-3}$) under

different culture conditions. Tukey's HSD test was then used to determine which conditions had different mRNA expression levels. *Tubb3* mRNA expression was significantly upregulated in cultures grown in the bioreactor ($p<6.5 \times 10^{-3}$), with the addition of K03861 ($p<4.11 \times 10^{-2}$) and with the addition of K03861 in the bioreactor ($p<1.33 \times 10^{-2}$) (**Figure 11**).

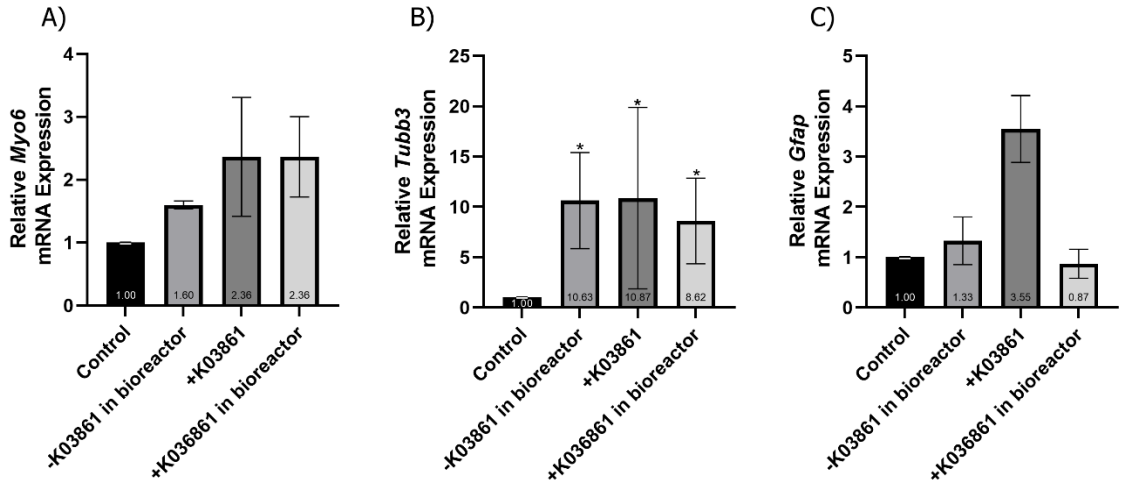

Fig. 11 Relative *Myo6, Tubb3,* and *Gfap* mRNA levels. Data was analyzed using one-way ANOVA and followed by Tukey's HSD. (A) No statistical significance was reported in levels of *Myo6* mRNA. (B) All culture conditions had a significant increase in *Tubb3* mRNA levels compared to control (C) No statistical significance was reported in levels of *Gfap* mRNA. Error bars indicate standard error.

Chapter 4: Discussion

Stem cell replacement therapy has the potential to replace loss or damaged hair cells to restore auditory function in patients with hearing loss. Stem cell replacement therapy requires efficient differentiation. Inadequate differentiation can diminish the efficacy of treating hearing loss while improper development can lead to teratoma formation. As a result, the objective of this study was to ensure commitment towards the hair cell fate and prevent teratoma formation as well as increase yields of sensory progenitors or differentiated hair cells in organoid cultures. We tested culture conditions in a bioreactor and addition of CDK2 inhibitor K03861 to achieve these goals.

bFGF withdrawal in iMOP cultures was previously used to promote cell cycle exit and drive sensory epithelial differentiation. Additional conditions were tested to improve the yield of MYO6 labeled cells, a marker for developing hair cells. iMOPs were cultured in four different conditions for sensory epithelial differentiation. The use of a bioreactor was incorporated to assist nutrient diffusion and CDK2 inhibitor K03861 was added to cultures to enrich for post-mitotic cells. This study reveals that the yield of MYO6 labeled cells can increase when iMOP cultures are grown in the bioreactor.

The use of a bioreactor increased the percentage of MYO6 labeled cells only in cultures without the addition of K03861. To determine whether the bioreactor facilitated differentiation for all three cell types, the proportions for neuronal marker TUBB3 and supporting cell marker GFAP were also assessed. The use of the bioreactor increased the proportion of TUBB3 labeled cells compared to control cultures, while the proportion of GFAP labeled cells was consistent throughout the different culture conditions.

While previous studies indicate that addition of K03861 increased the percentage of iMOP-derived neurons, no increase was observed for MYO6 labeled cells during sensory epithelial differentiation. K03861 inhibits CDK2 activity by competing with the cyclin binding site. Bound K03861 has a slow off-rate that prevents formation of an active cyclin-CDK complex. Addition of K03861 inhibits the formation of cyclin-CDK2 complexes to impede proliferation, enrich for cells that are stalled in the G1 phase of the cell cycle and allow accumulation of factors that may promote differentiation[36]. Active cyclin-CDK2 complexes promote progression of the G1/S phase in the cell cycle by phosphorylating many different proteins including CDKN1B (p27), a cyclin-dependent kinase inhibitor[47]. In addition to CDKN1B, there are many other proteins that could be phosphorylated by cyclin-CDK2. These phosphorylated targets may normally contribute to hair cell differentiation. Perhaps addition of K03861 could prevent phosphorylation of proteins that facilitate hair cell differentiation.

Transcript levels of *Myo6*, *Tubb3*, and *Gfap* in all four culture conditions were examined. RT-qPCR suggests that the vast majority of the samples did not mirror the increase in protein levels observed. Only cells cultured in the bioreactor showed a concomitant increase in both *Tubb3* transcript and TUBB3 protein. The differences between mRNA levels and protein expression among all four culture conditions is suggestive of additional post-translational mechanisms. This may explain the statistically insignificant differences in *Myo6* transcript levels in all culture conditions while an increased percentages of MYO6 labeled cells were seen in bioreactor cultures. Furthermore, RT-qPCR results are confounding since they represent average transcript levels from a heterogeneous population of cells from the organoids. The magnitude of

change is also dependent on the variable percentages of each cell type in the organoids. Results may be different if transcripts were obtained from specific cell types. The application of single-cell RNA sequencing may be a better approach to measure changes in the transcriptome of individual cells.

Ultimately, this study suggests that conditions supplied by the bioreactor may promote hair cell differentiation as observed by an increase in the percentage of MYO6 labeled cells compared to the previously established suspension culture condition. While bioreactor cultures show promising results in promoting hair cell differentiation, future studies will need to be conducted to further optimize hair cell maturation and function.

Chapter 5: References

1. Hu K. On Mammalian Totipotency: What Is the Molecular Underpinning for the Totipotency of Zygote?. *Stem Cells Dev*. 2019;28(14):897-906.
2. Kiecker C, Bates T, Bell E. Molecular specification of germ layers in vertebrate embryos. *Cell Mol Life Sci*. 2016;73(5):923-947.
3. Berdasco M, Esteller M. DNA methylation in stem cell renewal and multipotency. *Stem Cell Res Ther*. 2011;2(5):42. Published 2011 Oct 31.
4. Jung Y, Brack AS. Cellular mechanisms of somatic stem cell aging. *Curr Top Dev Biol*. 2014;107:405-438.
5. Takahashi K, Yamanaka S. Induction of pluripotent stem cells from mouse embryonic and adult fibroblast cultures by defined factors. *Cell*. 2006;126(4):663-676.
6. Marei, H.E., Althani, A., Lashen, S. *et al.* Genetically unmatched human iPSC and ESC exhibit equivalent gene expression and neuronal differentiation potential. *Sci Rep* **7,** 17504 (2017).
7. Arellano M, Moreno S. Regulation of CDK/cyclin complexes during the cell cycle. *Int J Biochem Cell Biol*. 1997;29(4):559-573.
8. Jablonska B, Aguirre A, Vandenbosch R, et al. Cdk2 is critical for proliferation and self-renewal of neural progenitor cells in the adult subventricular zone. *J Cell Biol*. 2007;179(6):1231-1245.
9. Liu L, Michowski W, Kolodziejczyk A, Sicinski P. The cell cycle in stem cell proliferation, pluripotency and differentiation. *Nat Cell Biol*. 2019;21(9):1060-1067.
10. Morrison, S., Kimble, J. Asymmetric and symmetric stem-cell divisions in development and cancer. *Nature* 441, 1068–1074 (2006).
11. Yang, Jienian et al. “The Role of Symmetric Stem Cell Divisions in Tissue Homeostasis.” *PLoS computational biology* vol. 11,12 e1004629. 23 Dec. 2015.
12. Yamashita YM, Yuan H, Cheng J, Hunt AJ. Polarity in stem cell division: asymmetric stem cell division in tissue homeostasis. *Cold Spring Harb Perspect Biol*. 2010;2(1):a001313.
13. Knoblich JA. Mechanisms of asymmetric stem cell division. *Cell*. 2008;132(4):583-597.
14. Catlin SN, Busque L, Gale RE, Guttorp P, Abkowitz JL. The replication rate of human hematopoietic stem cells in vivo. *Blood*. 2011;117(17):4460-4466.
15. Bretzner F, Gilbert F, Baylis F, Brownstone RM. Target populations for first-in-human embryonic stem cell research in spinal cord injury. *Cell Stem Cell*. 2011;8(5):468-475.
16. Mandai M, Kurimoto Y, Takahashi M. Autologous Induced Stem-Cell-Derived Retinal Cells for Macular Degeneration. *N Engl J Med*. 2017;377(8):792-793.

17. Takashima K, Inoue Y, Tashiro S, Muto K. Lessons for reviewing clinical trials using induced pluripotent stem cells: examining the case of a first-in-human trial for age-related macular degeneration. *Regen Med*. 2018;13(2):123-128.
18. Avior Y, Sagi I, Benvenisty N. Pluripotent stem cells in disease modelling and drug discovery. *Nat Rev Mol Cell Biol*. 2016;17(3):170-182.
19. Urbach A, Bar-Nur O, Daley GQ, Benvenisty N. Differential modeling of fragile X syndrome by human embryonic stem cells and induced pluripotent stem cells. *Cell Stem Cell*. 2010;6(5):407-411.
20. Blackwell DL, Lucas JW, Clarke TC. Summary health statistics for U.S. adults: National Health Interview Survey, 2012 (PDF). National Center for Health Statistics. Vital Health Stat 10(260). 2014.
21. National Research Council (US) Committee on Disability Determination for Individuals with Hearing Impairments; Dobie RA, Van Hemel S, editors. *Hearing Loss: Determining Eligibility for Social Security Benefits*. Washington (DC): National Academies Press (US); 2004. 2, Basics of Sound, the Ear, and Hearing.
22. Hudspeth AJ. Integrating the active process of hair cells with cochlear function. *Nat Rev Neurosci*. 2014;15(9):600-614.
23. Gillespie PG, Müller U. Mechanotransduction by hair cells: models, molecules, and mechanisms. *Cell*. 2009;139(1):33-44.
24. Purves D, Augustine GJ, Fitzpatrick D, et al., editors. Neuroscience. 2nd edition. Sunderland (MA): *Sinauer Associates*; 2001. Hair Cells and the Mechanoelectrical Transduction of Sound Waves.
25. Fritzsch B, Beisel KW, Hansen LA. The molecular basis of neurosensory cell formation in ear development: a blueprint for hair cell and sensory neuron regeneration?. *Bioessays*. 2006;28(12):1181-1193.
26. Wu DK, Kelley MW. Molecular mechanisms of inner ear development. *Cold Spring Harb Perspect Biol*. 2012;4(8):a008409. Published 2012 Aug 1.
27. Gálvez H, Tena JJ, Giraldez F, Abelló G. The Repression of Atoh1 by Neurogenin1 during Inner Ear Development. *Front Mol Neurosci*. 2017;10:321. Published 2017 Oct 20.
28. Gálvez H, Abelló G, Giraldez F. Signaling and Transcription Factors during Inner Ear Development: The Generation of Hair Cells and Otic Neurons. *Front Cell Dev Biol*. 2017;5:21. Published 2017 Mar 24.
29. Ma Q, Anderson DJ, Fritzsch B. Neurogenin 1 null mutant ears develop fewer, morphologically normal hair cells in smaller sensory epithelia devoid of innervation [published correction appears in *J Assoc Res Otolaryngol* 2000 Dec;1(4):326]. *J Assoc Res Otolaryngol*. 2000;1(2):129-143.
30. Stone JS, Cotanche DA. Hair cell regeneration in the avian auditory epithelium. *Int J Dev Biol*. 2007;51(6-7):633-647.
31. Mulvaney J, Dabdoub A. Atoh1, an essential transcription factor in neurogenesis and intestinal and inner ear development: function, regulation, and context dependency. *J Assoc Res Otolaryngol*. 2012;13(3):281-293.

32. Lalwani AK, Walsh BJ, Reilly PG, Muzyczka N, Mhatre AN. Development of in vivo gene therapy for hearing disorders: introduction of adeno-associated virus into the cochlea of the guinea pig. *Gene Ther*. 1996;3(7):588-592.
33. Murine ESCs stepwise differentiation
34. Chen J, Hong F, Zhang C, et al. Differentiation and transplantation of human induced pluripotent stem cell-derived otic epithelial progenitors in mouse cochlea. *Stem Cell Res Ther*. 2018;9(1):230. Published 2018 Aug 29.
35. Groves AK. The challenge of hair cell regeneration. *Exp Biol Med (Maywood)*. 2010;235(4):434-446.
36. Azadeh J, Song Z, Laureano AS, Toro-Ramos A, Kwan K. Initiating Differentiation in Immortalized Multipotent Otic Progenitor Cells. *J Vis Exp*. 2016;(107):53692. Published 2016 Jan 2.
37. Kwan KY, Shen J, Corey DP. C-MYC transcriptionally amplifies SOX2 target genes to regulate self-renewal in multipotent otic progenitor cells. *Stem Cell Reports*. 2015;4(1):47-60.
38. Latremoliere A, Cheng L, DeLisle M, et al. Neuronal-Specific TUBB3 Is Not Required for Normal Neuronal Function but Is Essential for Timely Axon Regeneration. *Cell Rep*. 2018;24(7):1865-1879.e9.
39. Hol EM, Pekny M. Glial fibrillary acidic protein (GFAP) and the astrocyte intermediate filament system in diseases of the central nervous system. *Curr Opin Cell Biol*. 2015;32:121-130.
40. Self T, Sobe T, Copeland NG, Jenkins NA, Avraham KB, Steel KP. Role of myosin VI in the differentiation of cochlear hair cells. *Dev Biol*. 1999;214(2):331-341.
41. Liu M, Liu N, Zang R, Li Y, Yang ST. Engineering stem cell niches in bioreactors. World J Stem Cells. 2013;5(4):124-135. doi:10.4252/wjsc.v5.i4.124
42. King JA, Miller WM. Bioreactor development for stem cell expansion and controlled differentiation. *Curr Opin Chem Biol*. 2007;11(4):394-398.
43. Han S, Yang K, Shin Y, et al. Three-dimensional extracellular matrix-mediated neural stem cell differentiation in a microfluidic device. *Lab Chip*. 2012;12(13):2305-2308.
44. Song Z, Jadali A, Fritzsch B, Kwan KY. NEUROG1 Regulates CDK2 to Promote Proliferation in Otic Progenitors. *Stem Cell Reports*. 2017;9(5):1516-1529.
45. Alexander LT, Möbitz H, Drueckes P, et al. Type II Inhibitors Targeting CDK2. *ACS Chem Biol*. 2015;10(9):2116-2125.
46. Romero-Morales, A. I., O'Grady, B. J., Balotin, K. M., Bellan, L. M., Lippmann, E. S., & Gama, V. Spin∞ an improved miniaturized spinning bioreactor for the generation of human cerebral organoids from pluripotent stem cells. *HardwareX*. 2009;*6*(e00082).
47. Abbastabar M, Kheyrollah M, Azizian K, et al. Multiple functions of p27 in cell cycle, apoptosis, epigenetic modification and transcriptional regulation for the control of cell growth: A double-edged sword protein. *DNA Repair (Amst)*. 2018;69:63-72.